NOVEL DESIGN OF STACKED DUAL LAYER STRIP LINES FED WIDEBAND PATCH ANTENNA FOR GNSS APPLICATION

Xi Li*, Lin Yang, and Qiong Chen

National Laboratory of Science and Technology on Antennas and Microwaves, Xidian University, Xi'an, Shaanxi, China

Abstract—This paper presents a novel design of stacked dual layer strip lines fed patch antenna. The wideband characteristics can be achieved by employing approximate L-probes coupling feeding schemes. Dual layer strip lines which are composed of one broadband 180° hybrid and two wideband 90° hybrids are introduced as feeding network in this design. As a result, the designed antenna has a 59.4% 10-dB input reflection coefficient bandwidth and 48.3% 3-dB axial ratio (AR) bandwidth relative to the center frequency respectively. The designed antenna occupies a compact size of 80 mm × 80 mm × 32 mm. The final antenna provides a very good circularly polarized radiation for Global Navigation Satellite System applications including GPS, GLONASS, Galileo and Compass.

1. INTRODUCTION

With the development of global navigation satellite system (GNSS), the requests for multi-system navigation ability increase. To fulfill the need, the antennas should have characteristics of wideband, stable gain bandwidth, broad beamwidth, low cross-polarization at low elevation and compact size.

Recently, GNSS antenna has become a popular topic of research, and lots of GNSS antennas have been proposed, including microstrip patch antennas, quadrifilar helix antenna, dielectric resonant antennas and Spiral antennas. Spiral antennas have frequency-independent impedance and radiation performance [1]. However, spiral antennas usually need a cavity reflector, which makes them heavy and bulky. Quadrifilar helical antenna has exciting radiation characteristics of

broad beam-width [2, 3], but the disadvantages of big size and narrow bandwidth limit its applications. Microstrip patch antennas [4–20] are good candidates of GNSS antennas because of their advantages of low-profile, low cost, easy fabrication and compatibility with integrated circuit technology. However, the general limitations of the traditional microstrip antennas are achievable impedance and axial-ratio (AR) bandwidths. There are many methods to achieve broadband performance of microstrip antennas, such as using two or more radiating structures which work at different but contiguous resonant frequencies, using coupling feeding scheme, adding external matching circuits and so on. Several multi-band or wideband low-profile antennas have been proposed in the literature [8–11, 21] for GPS or GNSS application. However, few of them can provide broad beamwidth and low cross-polarization at low elevation, which are useful to suppressing multipath interferences.

Our goal is designing a broadband antenna that covering all the GNSS frequencies, and the antenna can maintain stable, high performance at all the frequencies. In this paper, a novel design of stacked dual layer strip lines fed patch antenna is presented for GNSS application. The presented antenna can be characterized by the following features: 1) printed approximate L-probes connected to broadband 180° and 90° hybrids are used as feeding schemes, which can easily obtain wideband impedance and AR bandwidths. 2) Dual layer strip lines are introduced in this design. In this case, the size of the feeding network can be greatly reduced and the antenna can be fed by an SMA connector from the bottom of substrate, which is propitious to feeding the array. 3) The feeding network is arranged along the diagonal of the substrate, helping to optimize the space utilization. 4) The crossed slots are cut on the radiating patch, which can increase the antenna gain. 5) The designed antenna has characteristics of broad beamwidth and good cross-polarization at low elevation, which are useful to suppressing multipath interferences.

In the next section, the antenna configuration and design principle are described. The simulated and measured results of the antenna are depicted in results and discussion section, followed by a brief conclusion.

2. ANTENNA CONFIGURATION AND DESIGN

Figure 1 shows structure of the proposed stacked dual layer strip lines fed patch antenna. The antenna design includes four layers. The radiating patch is printed on the top of the first substrate, and the crossed slots have been cut on the radiating patch to increase the
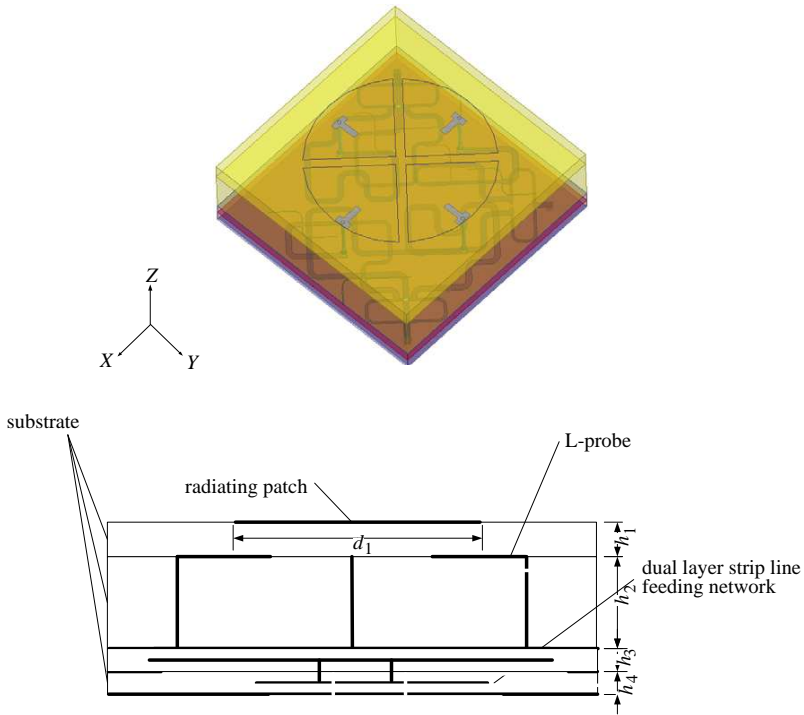
Figure 1. The structure of the proposed antenna.
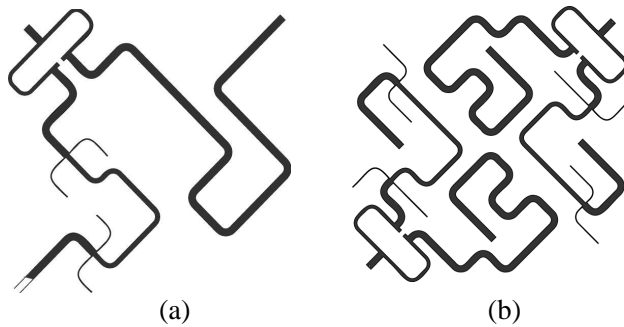

Figure 2. The construction of the feeding network. (a) Broadband 180° hybrid. (b) Broadband 90° hybrids.

antenna gain. Four approximate L-probes include four metal strips which are printed on the top of the second substrate and the posts, which go through the substrate and are connected to the broadband 90°
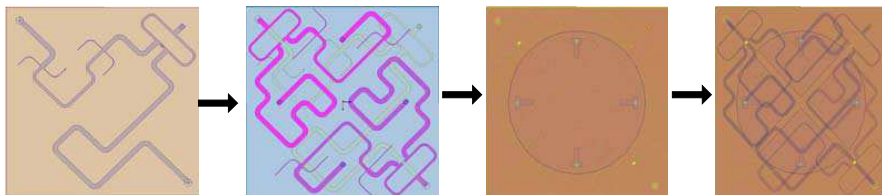
Figure 3. The design procedure of the proposed antenna.
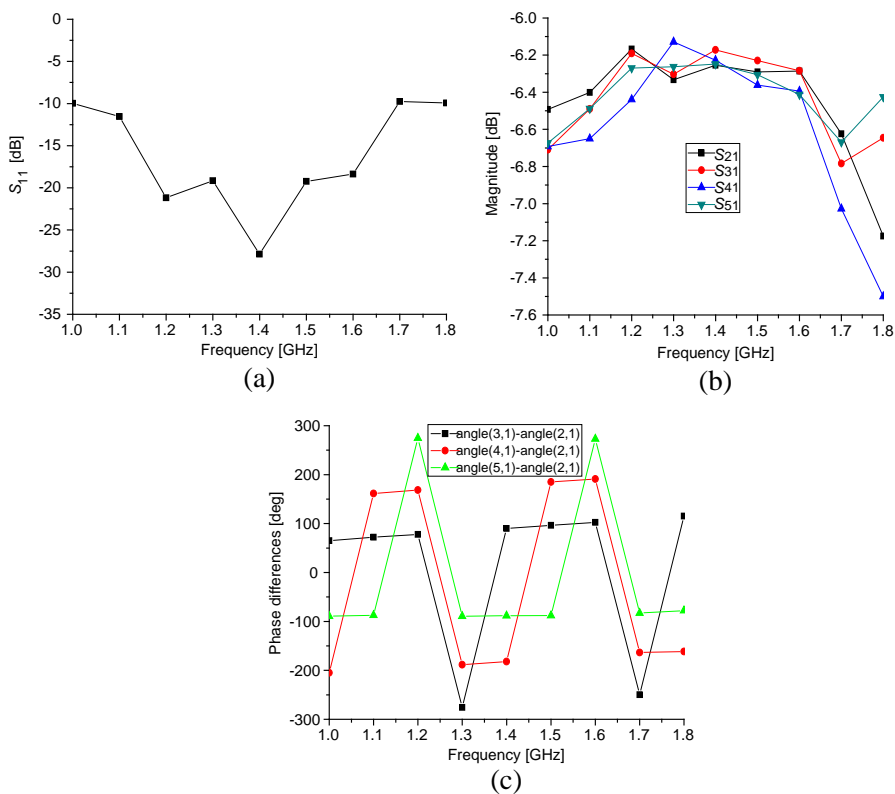

(a)

(b)

(c)

Figure 4. Simulated performances of the feeding network. (a) Simulated input reflection coefficient of the feeding network. (b) Simulated magnitude response of the feeding network. (c) Simulated phase differences of the feeding network.

hybrid ports. The dimensions of the probes and the distances between strips and radiating patch affect the coupling effect. The third layer and the fourth layer are the substrate layer of the strip lines feeding network, which is composed of one broadband 180° and two wideband 90° hybrids. In this case, the feeding network can provide good 90° phase differences between two adjacent ports. The configuration of the feeding network is shown in Figure 2.

Figure 3 shows the design procedure of the proposed antenna. At first, the broadband 180° strip line hybrid is designed and optimized as primary feeding network and is located at the fourth layer; then two wideband 90° strip line hybrids are connected to the 180° hybrid by probes and located at the third layer. The whole feeding network is optimized to obtain small magnitude variation and phase shift unbalance; then the circular patch is designed as radiating patch to work at GNSS bands. The height of the second layer (h_2) is optimized to obtain the widest VSWR bandwidth, and at last, the crossed slots are cut on the radiating patch to increase the antenna gain. Figure 4 displays the simulated input reflection coefficient, magnitude response and phase differences of the feeding network using HFSS ver.13 [23]. We observe that the magnitude variation is less than 0.3 dB and the phase shift unbalance is less than 5° in the band of 1.1–1.6 GHz.

The key dimensions of the structure are as follows: $L = 80$ mm (length of the substrate), $\varepsilon_r = 4.4$ (permittivity of all substrate), $d_1 = 60$ mm (outer diameter of the radiating patch), $h_1 = 6$ mm (height of the first substrate), $h_2 = 18$ mm (height of the second substrate layer), $h_3 = 4$ mm (height of the third strip lines substrate layer), $h_4 = 4$ mm (height of the fourth strip lines substrate layer).

3. RESULTS AND DISCUSSION

The input reflection coefficient, axial ratio, radiation pattern and gain of the final fabricated antenna have been simulated and measured. Figure 5 presents the variety of input reflection coefficient affected by the dimensions of h_2. As can be seen in the figure, when $h_2 = 18$ mm, the antenna can acquire the widest impedance bandwidth. Figure 6 compares simulated RHCP gain of the proposed antenna including crossed slots with that without crossed slots. Obviously, the structure including crossed slots can increase the antenna gain. It's mainly because the radiation efficiency of the proposed antenna with crossed slots can be greatly improved compared with that without crossed slots, which can be seen from Figure 7. Figure 8 also depicts the variety of antenna gain affected by the width of slots (ws). From the figure, when increasing the value of ws, the antenna gain at high

frequencies increases, oppositely, the antenna gain at low frequencies decreases, but it is not very clearly. Finally, we choose ws as $3\,mm$ because that in the GNSS band ($1.1\,GHz$–$1.6\,GHz$), the antenna gains are a little higher than the other ws values. Figure 9 shows the photo of the fabricated antenna. The overall size of the antenna is $80\,mm \times 80\,mm \times 32\,mm$, whose transverse dimensions are smaller than the literature [9–11]. The measured input reflection coefficient collected from Agilent E8363B network analyzer along with simulated results using HFSS are presented in Figure 10, the deviations between them are mainly due to machine errors and mount errors. It can be observed that the measured impedance bandwidth for $S_{11} < -10\,dB$ is 59.4%, ranging from 1.03 to $1.9\,GHz$.
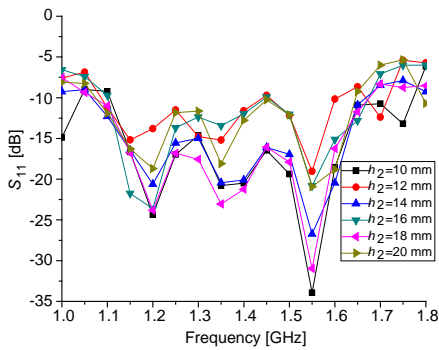
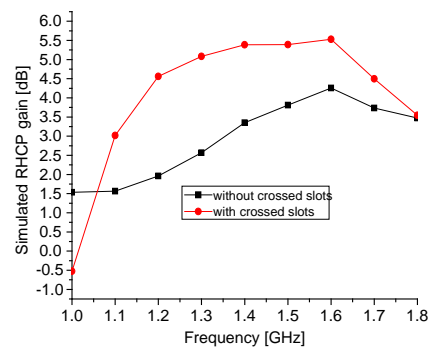**Figure 5.** Simulated input reflection coefficient of the proposed antenna for various h_2.

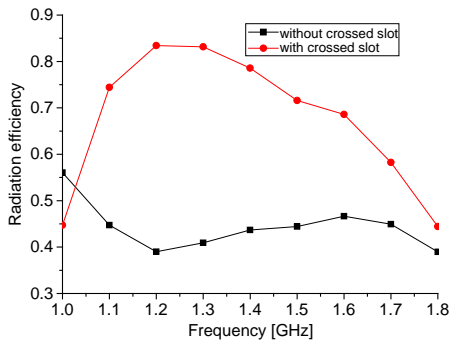**Figure 6.** Simulated RHCP gain of the proposed antenna with and without crossed slots.

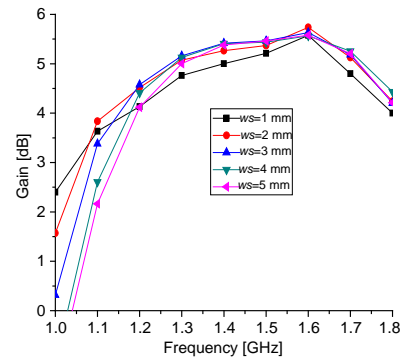**Figure 7.** The radiation efficiency with and without crossed slots

Figure 8. Simulated antenna gain for various ws.
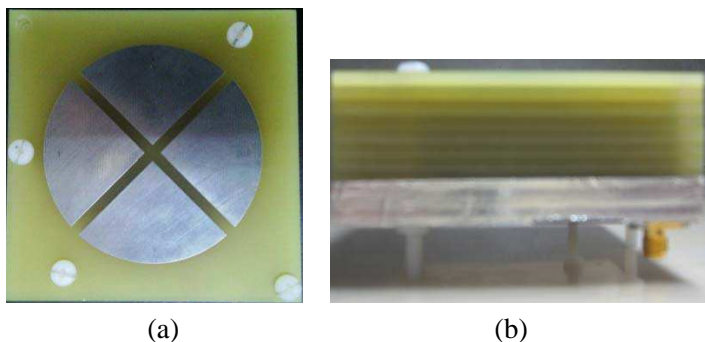
(a)   (b)

Figure 9. The photo of the proposed antenna. (a) Front view. (b) Side view.
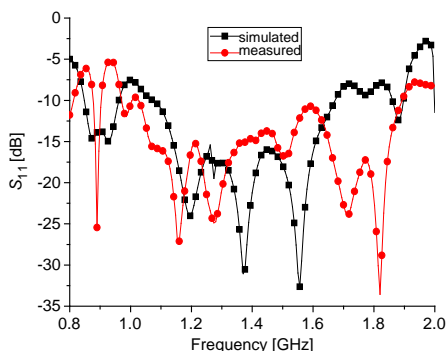

Figure 10. Simulated and measured input reflection coefficient of the proposed antenna.
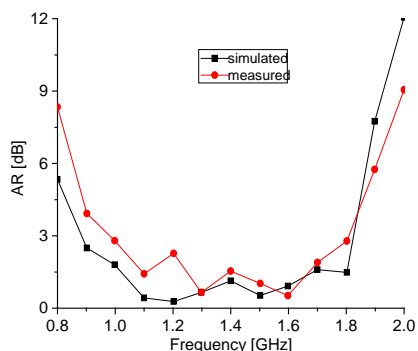
Figure 11. Simulated and measured AR.

The radiation performances were measured in an anechoic chamber. Two Archimedean spiral antennas were used to measure right-hand circular polarization and left-hand circular polarization radiation, respectively. Figure 11 depicts the simulated and measured AR at $+Z$ direction, the 3-dB AR bandwidths of the proposed antenna is 48.3% from 1.0 to 1.8 GHz. As can be seen in the figure, the impedance and AR bandwidths are sufficient to cover GNSS frequencies. The measured AR patterns in the X-Z and Y-Z planes at 1.2, 1.4 and 1.6 GHz are presented in Figure 12. As seen, the elevation angles for AR $<$ 5 dB are $-90°$–$90°$ at X-Z plane and $-91°$–$96°$ at Y-Z plane respectively at 1.2 GHz, $-104°$–$104°$ at X-Z plane and $-110°$–$110°$ at Y-Z plane respectively at 1.4 GHz, $-120°$–$120°$ at X-Z
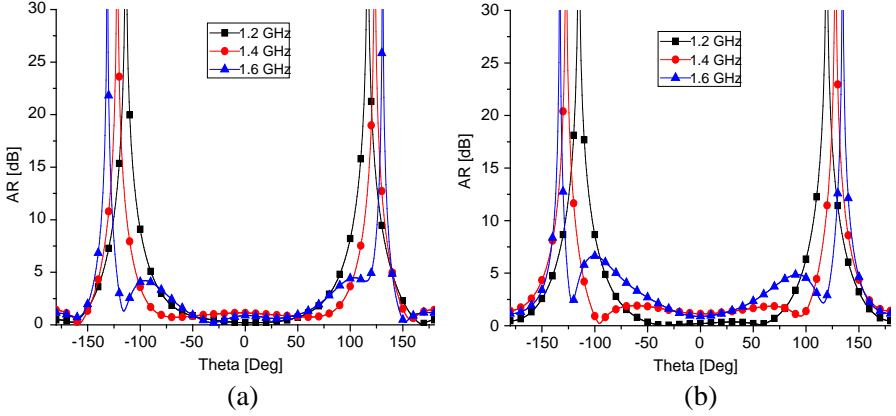
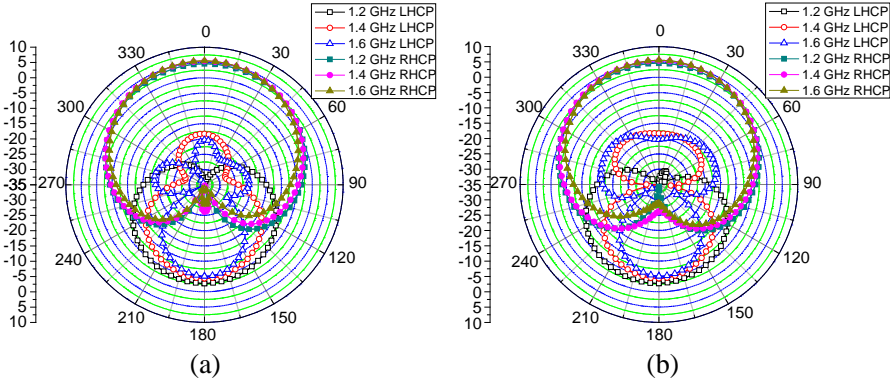**Figure 12.** Measured AR patterns. (a) *X-Z* plane. (b) *Y-Z* plane.

Figure 13. Measured radiation patterns. (a) *X-Z*. (b) *Y-Z*.

plane and $-80°$–$124°$ at *Y-Z* plane respectively at 1.6 GHz. Figure 13 shows the measured radiation patterns in the *X-Z* and *Y-Z* planes at three different frequencies 1.2, 1.4 and 1.6 GHz. Broad pattern coverage and high gain at low elevation angles (more than -5 dBi at elevation angles $> 10°$) is achieved. The excellent performances of the antenna are mainly due to stacked dual layer structure and four ports proximity-coupled probe-fed feeding mechanism. Cross-polarization and gain characteristics at low elevation are better than literatures [8–12, 21, 22]. The simulated and measured RHCP gains of the antenna are presented in Figure 14, and it is observed that the stable gain bandwidth can be obtained for gain > 2 dBi.
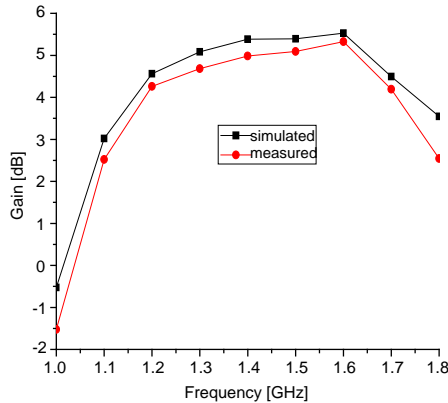
Figure 14. Simulated and measured gain of the proposed antenna.

4. CONCLUSION

This paper presents a novel design of circularly polarized patch antenna for GNSS application with size of 80 mm × 80 mm × 32 mm. A dual layer strip lines feeding structure is introduced in this design to compact the transverse dimensions. Using the proposed structure, the antenna exhibits an effective bandwidth of 48.3% from 1.1 to 1.8 GHz for $S_{11} < -10$ dB and AR < 3 dB. Moreover, the proposed antenna can obtain stable gain bandwidths, broad beamwidth and good cross-polarization at low elevation characteristics. Measured parameters show good agreement with the modeling and conform that such antennas can be successfully used for GNSS applications.

ACKNOWLEDGMENT

REFERENCES

1. Kramer, B. A., S. Koulouridis, C. C. Chen, and J. L. Volakis, "A novel reflective surface for an UHF spiral antenna," *IEEE Antennas and Wireless Propagation Letters*, Vol. 5, 32–34, 2006.

2. Kilgus, C., "Resonant quadrifilar helix," *IEEE Transactions on Antennas and Propagation*, Vol. 17, No. 3, 349–351, 1969.

3. Amin, M. and R. Cahill, "Compact quadrifilar helix antenna," *Electronics Letters*, Vol. 41, 672–674, 2005.

4. Huang, J. and V. Jamnejad, "A microstrip array feed for land mobile satellite reflector antennas," *IEEE Transactions on Antennas and Propagation*, Vol. 37, No. 2, 153–158, 1989.

5. Chebolu, S., S. Dey, R. Mittra, and M. Itoh, "A dual-band stacked microstrip antenna array for mobile satellite applications," *Antennas and Propagation Society International Symposium, AP-S. Digest*, Vol. 1, 598–601, 1995.

6. Wu, J. Y., J. S. Row, and K. L. Wong, "A compact dual-band microstrip patch antenna suitable for DCS/GPS operations," *Microwave and Optical Technology Letters*, Vol. 29, No. 6, 410–412, 2001.

7. Guo, Y. X., L. Bian, and X. Q. Shi, "Broadband circularly polarized annular-ring microstrip antenna," *IEEE Transactions on Antennas and Propagation*, Vol. 57, No. 8, 2474–2477, 2009.

8. Zhou, Y., C. C. Chen, and J. L. Volakis, "Dual band proximity-fed stacked patch antenna for tri-band GPS applications," *IEEE Transactions on Antennas and Propagation*, Vol. 55, No. 1, 220–223, Jan. 2007.

9. Wang, Z. B., S. J. Fang, S. Q. Fu, and S. W. Lu, "Dual-band probe-fed stacked patch antenna for GNSS applications," *IEEE Antennas and Wireless Propagation Letters*, Vol. 8, 100–103, 2009.

10. Pimenta, M. S., F. Ferrero, R. Staraj, and J. M. Ribero, "Low-pofile circularly polarized GNSS antenna," *Microwave and Optical Technology Letters*, Vol. 54, No. 12, 2811–2814, 2012.

11. Ma, J. P., A. B. Kouki, and R. Landry, Jr., "Wideband circularly polarized single probe-fed patch anteena," *Microwave and Optical Technology Letters*, Vol. 54, No. 8, 1803–1808, 2012.

12. Moernaut, G. J. K. and G. A. E. Vandenbosch, "Concept study of a shorted annular patch antenna: Design and fabrication on a conducting cylinder," *IEEE Transactions on Antennas and Propagation*, Vol. 59, No. 1, 2097–2102, Jan. 2011.

13. Kasabegoudar, V. G. and K. J. Vinoy, "A broadband suspended microstrip antenna for circular polarization," *Progress In Electromagnetics Research*, Vol. 90, 353–368, 2009.

14. Bao, X. L. and M. J. Ammann, "Comparison of several novel annular-ring microstrip patch antennas for circular polarization," *Journal of Electromagnetic Waves and Applications*, Vol. 20, No. 20, 1427–1438, 2006.

15. Liu, W. C. and P. C. Kao, "Design of a probe-fed H-

shaped microstrip antenna for circular polarization," *Journal of Electromagnetic Waves and Applications*, Vol. 21, No. 7, 857–864, 2007.

16. Chang, T. N. and J. H. Jiang, "Enhance gain and bandwidth of circularly polarized microstrip patch antenna using gap-coupled method," *Progress In Electromagnetics Research*, Vol. 96, 127–139, 2009.

17. Heidari, A. A., M. Heyrani, and M. Nakhkash, "A dual-band circularly polarized stub loaded microstrip patch antenna for GPS applications," *Progress In Electromagnetics Research*, Vol. 92, 195–208, 2009.

18. Yang, S. S., K.-F. Lee, A. A. Kishk, and K.-M. Luk, "Design and study of wideband single feed circularly polarized microstrip antennas," *Progress In Electromagnetics Research*, Vol. 80, 45–61, 2008.

19. Wu, G.-L., W. Mu, G. Zhao, and Y.-C. Jiao, "A novel design of dual circularly polarized antenna fed by L-strip," *Progress In Electromagnetics Research*, Vol. 79, 39–46, 2008.

20. Yu, A., F. Yang, and A. Z. Elsherbeni, "A dual band circularly polarized ring antenna based on composite right and left handed metamaterials," *Progress In Electromagnetics Research*, Vol. 78, 73–81, 2008.

21. Zhou, Y., S. Koulouridis, G. Kizitas, and J. L. Volakis, "A novel 1.5″ quadruple antenna for tri-band GPS applications," *IEEE Antennas and Wireless Propagation Letters*, Vol. 5, 224–227, 2006.

22. Zheng, L. and S. Gao, "Compact dual-band printed square quadrfilar helix antenna for global navigation satellite system receivers," *Microwave and Optical Technology Letters*, Vol. 53, No. 5, 993–997, 2011.

23. "Ansoft high frequency structure simulation (HFSS)," Ver. 13, ANSYS, Inc., Canonsburg, PA, 2011.